Intensity noise correlations in a two-frequency VECSEL

S. De,[1] V. Pal,[2] A. El Amili,[1,3] G. Pillet,[4] G. Baili,[4] M. Alouini,[3,4] I. Sagnes,[5] R. Ghosh,[2,6] and F. Bretenaker[1,*]

[1]*Laboratoire Aimé Cotton, CNRS-Université Paris Sud 11, Campus d'Orsay, 91405 Orsay Cedex, France*
[2]*School of Physical Sciences, Jawaharlal Nehru University, New Delhi 110067, India*
[3]*Institut de Physique de Rennes, UMR CNRS 6251, Campus de Beaulieu, 35042 Rennes Cedex, France*
[4]*Thales Research & Technology, 1 av. Augustin Fresnel, 91767 Palaiseau Cedex, France*
[5]*Laboratoire de Photonique et Nanostructures, CNRS, Route de Nozay, 91460 Marcoussis, France*
[6]*School of Natural Sciences, Shiv Nadar University, Gautam Budh Nagar, UP 203207, India*
[*]*Fabien.Bretenaker@u-psud.fr*

Abstract: We present an experimental and theoretical study of the intensity noise correlation between the two orthogonally polarized modes in a dual frequency Vertical External Cavity Surface Emitting Laser (VECSEL). The dependence of the noise correlation spectra on the non-linear coupling between the two orthogonally polarized modes is put into evidence. Our results show that for small coupling the noise correlation amplitude and phase spectra remain nearly flat (around -6 dB and 0^o respectively) within the frequency range of our interest (from 100 kHz to 100 MHz). But for higher values of the coupling constant the low frequency behaviors (below 1-2 MHz) of the correlation amplitude and phase spectra are drastically changed, whereas above this cut-off frequency (1-2 MHz) the correlation spectra are almost independent of coupling strength. The theoretical model is based on the assumptions that the only source of noise in the frequency range of our interest for the two modes are pump noises, which are white noises of equal amplitude but partially correlated.

OCIS codes: (140.7260) Vertical cavity surface emitting lasers; (270.2500) Fluctuations, relaxations, and noise.

References and links

1. M. Alouini, B. Benazet, M. Vallet, M. Brunel, P. Di Bin, F. Bretenaker, A. Le Floch, and P. Thony, "Offset phase locking of Er:Yb:Glass laser eigenstates for RF photonics applications," IEEE Photon. Technol. Lett. **13**, 367–369 (2001).
2. S. Tonda-Goldstein, D. Dolfi, A. Monsterleet, S. Formont, J. Chazelas, and J.-P. Huignard, "Optical signal processing in radar systems," IEEE Trans. Microwave Theory and Techniques **54**, 847-853 (2006).
3. G. Pillet, L. Morvan, M. Brunel, F. Bretenaker, D. Dolfi, M. Vallet, J.-P. Huignard, and A. Le Floch, "Dual frequency laser at 1.5 μm for optical distribution and generation of high-purity microwave signals," J. Lightwave Technol. **26**, 2764-2773 (2008).
4. L. Morvan, N. D. Lai, D. Dolfi, J.-P. Huignard, M. Brunel, F. Bretenaker, and A. Le Floch, "Building blocks for a two-frequency laser lidar-radar: a preliminary study," Appl. Opt. **41**, 5702-5712 (2002).
5. M. Brunel, F. Bretenaker, and A. Le Floch, "Tunable optical microwave source using spatially resolved laser eigenstates," Opt. Lett. **22**, 384-386 (1997).

#178129 - $15.00 USD Received 16 Oct 2012; revised 14 Jan 2013; accepted 15 Jan 2013; published 28 Jan 2013

6. M. Alouini, M. Brunel, F. Bretenaker, M. Vallet, and A. Le Floch, "Dual tunable wavelength Er:Yb:Glass laser for terahertz beat frequency generation," IEEE Photon. Technol. Lett. **10**, 1554–1556 (1998).
7. R. Czarny, M. Alouini, C. Larat, M. Krakowski, and D. Dolfi, "THz-dual-frequency Yb^{3+}:$KGd(WO_4)_2$ laser for continuous wave THz generation through photomixing," Electron. Lett. **40**, 942-943 (2004).
8. F. T. Arecchi, G. L. Lippi, G. P. Puccioni, and J. R. Tredicce, "Deterministic chaos in laser with injected signal," Opt. Commun. **51**, 308-314 (1984).
9. S. Taccheo, P. Laporta, O. Svelto, and G. de Geronimo, "Intensity noise reduction in a single-frequency ytterbium-codoped erbium laser," Opt. Lett. **21**, 1747-1749 (1996).
10. G. Baili, L. Morvan, M. Alouini, D. Dolfi, F. Bretenaker, I. Sagnes, and A. Garnache, "Experimental demonstration of a tunable dual-frequency semiconductor laser free of relaxation oscillations," Opt. Lett. **34**, 3421-3423 (2009).
11. M. Sargent III, M. O. Scully, and W. E. Lamb, Jr., *Laser Physics* (Addison-Wesley, 1974).
12. M. M.-Tehrani and L. Mandel, "Coherence theory of the ring laser," Phys. Rev. A **17**, 677-693 (1978).
13. V. Pal, P. Trofimoff, B.-X. Miranda, G. Baili, M. Alouini, L. Morvan, D. Dolfi, F. Goldfarb, I. Sagnes, R. Ghosh, and F. Bretenaker, "Measurement of the coupling constant in a two-frequency VECSEL," Opt. Express **18**, 5008-5014 (2010).
14. M. San Miguel, Q. Feng, and J. V. Moloney, "Light-polarization dynamics in surface-emitting semiconductor lasers," Phys. Rev. A **52**, 1728-1739 (1995).
15. J. Martin-Regalado, M. San Miguel, N. B. Abraham, and F. Prati, "Polarization switching in quantum-well vertical-cavity surface-emitting lasers," Opt. Lett. **21**, 351-353 (1996).
16. M. Travagnin, M. P. van Exter, and J. P. Woerdman, "Influence of carrier dynamics on the polarization stability and noise-induced polarization hopping in surface-emitting semiconductor lasers," Phys. Rev. A **56**, 1497-1507 (1997).
17. G. Baili, F. Bretenaker, M. Alouini, L. Morvan, D. Dolfi, and I. Sagnes, "Experimental investigation and analytical modeling of excess intensity noise in semiconductor class-A lasers," J. Lightwave Technol. **26**, 952-961 (2008).
18. A. Laurain, M. Myara, G. Beaudoin, I. Sagnes, and A. Garnache, "High power single–frequency continuously–tunable compact extended–cavity semiconductor laser," Opt. Express **17,** 9503–9508 (2009).
19. G. Baili, M. Alouini, D. Dolfi, F. Bretenaker, I. Sagnes, and A. Garnache, "Shot-noise-limited operation of a monomode high-cavity-finesse semiconductor laser for microwave photonics applications," Opt. Lett. **32**, 650-652 (2007).
20. G. Baili, M. Alouini, T. Malherbe, D. Dolfi, I. Sagnes, and F. Bretenaker, "Direct observation of the class-B to class-A transition in the dynamical behavior of a semiconductor laser," Europhys. Lett. **87**, 44005 (2009).
21. D. E. McCumber, "Intensity fluctuations in the output of cw laser oscillators. I," Phys. Rev. **141**, 306-322 (1966).
22. K. Otsuka, P. Mandel, S. Bielawski, D. Derozier, and P. Glorieux, "Alternate time scale in multimode lasers," Phys. Rev. A **46**, 1692-1695 (1992).
23. C. H. Henry, "Theory of the linewidth of semiconductor lasers," IEEE J. Quantum Electron. **18**, 259-264 (1982).
24. C. H. Henry, "Phase noise in semiconductor laser," J. Lightwave. Technol. **4**, 298-311 (1986).

1. Introduction

Optical generation, transport, or processing of radio-frequency (RF) signals becomes more and more important for many applications. For example, these RF signals are essential for long range transmission of high purity RF references [1] and wide-band radar signal processing [2]. Rather than modulating a single-frequency laser or beating two separate lasers, the direct generation of an optically carried RF beat note in a two-frequency laser is a promising strategy for the optical distribution and generation of radar local oscillators [3], and for pulsed or CW lidar-radar systems [4]. Such dual frequency operation has been demonstrated for diode pumped solid-state lasers, e.g., Nd:YAG [5], Er:Yb:Glass [6] and Yb^{3+}:KGW lasers [7]. However, the main limitation of these solid-state two-frequency lasers lies in their relatively strong intensity noise inherent to their class-B dynamical behavior [8,9]. This is the reason why dual-frequency operation has recently been demonstrated in a class-A VECSEL, since such two-frequency VECSELs do not suffer from relaxation oscillations. This is due to the fact that the photon lifetime inside the cavity is much longer than the excited carriers lifetime, thus ensuring the class-A dynamical behavior of the VECSELs [10]. The two-frequency operation of VECSEL has also other advantages since the two oscillating polarized modes share the same cavity. As a result the frequency difference between the two modes can be tuned by changing the intra-

#178129 - $15.00 USD Received 16 Oct 2012; revised 14 Jan 2013; accepted 15 Jan 2013; published 28 Jan 2013

cavity phase anisotropy. Moreover the two mode fields are expected to exhibit highly correlated phase and intensity fluctuations. However, it is important to remember that the simultaneous oscillation of the two modes relies on the value of the non-linear coupling constant between the modes, which should be less than unity [11–13]. In dual-frequency VECSELs, the coupling constant value is reduced by spatially separating the two orthogonally polarized modes on the gain structure with a intra-cavity birefringent crystal. Our aim here is thus to theoretically and experimentally investigate the intensity noise of such a two-frequency VECSEL. More precisely, we aim at measuring the intensity noise spectra and intensity noise correlations between the two modes, and to investigate how the coupling constant between the two modes can alter these noise characteristics. We focus on the frequency range between 100 kHz and 100 MHz, where the dominant source of intensity noise is the pump laser noise. To this aim, we describe in Sec. 2 the theoretical model that we have developed to describe the influence of this pump noise on the intensity noise of the VECSEL. Section 3 describes the experimental setup and how we measure noise correlations between the modes. In Sec. 4, the predictions of the model are compared with the experimental results obtained for different values of the coupling between the two modes. We then attempt to give a physical picture of the results in Sec. 5.

2. Theoretical Model

In this section, we aim at deriving a theoretical model to predict how the pump intensity noise is transferred to the intensity noise of our dual-frequency VECSEL. In our laser, the two modes are cross-polarized and are spatially separated in the active medium thanks to an intra-cavity birefringent crystal, as sketched in Fig. 1. This leads to a partial overlap of the two modes in the active medium.

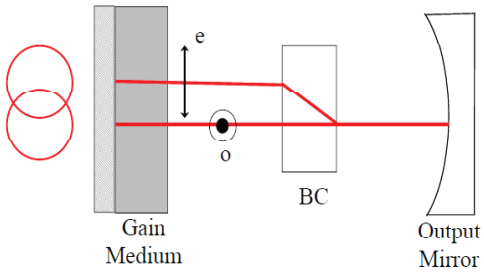

Fig. 1. Schematic representation of the considered two-frequency laser. The ordinary (o) and extraordinary (e) polarized modes are partially spatially separated in the active medium thanks to the birefringent crystal BC.

To model this laser, we chose to write the simplest possible rate equations governing the time evolution of the photon numbers F_1 and F_2 in the two modes. Moreover, we suppose that these two modes have two corresponding population inversions N_1 and N_2, with some partial overlap between the two modes. This approach has the advantage of being very simple and of allowing us to introduce the possibility to vary the coupling constant by changing the spatial overlap between the modes in a very simple way. For comparison, introducing this varying spatial overlap between the modes in the spin-flip model [14–16] would not be straightforward

#178129 - $15.00 USD Received 16 Oct 2012; revised 14 Jan 2013; accepted 15 Jan 2013; published 28 Jan 2013

at all. The rate equations that we use thus read:

$$\frac{dF_1(t)}{dt} = -\frac{F_1}{\tau_1} + \kappa N_1 F_1, \quad (1)$$

$$\frac{dF_2(t)}{dt} = -\frac{F_2}{\tau_2} + \kappa N_2 F_2, \quad (2)$$

$$\frac{dN_1(t)}{dt} = \frac{1}{\tau}(N_{01} - N_1) - \kappa N_1 (F_1 + \xi_{12} F_2), \quad (3)$$

$$\frac{dN_2(t)}{dt} = \frac{1}{\tau}(N_{02} - N_2) - \kappa N_2 (F_2 + \xi_{21} F_1), \quad (4)$$

where τ_1 and τ_2 are the photon lifetimes inside the cavity for the two modes, which we suppose to be different if the two modes have slightly different losses. τ is the population inversion lifetime which is identical for both the modes. N_{01}/τ and N_{02}/τ are the pumping rates for the two modes. Thus N_{01} and N_{02} denote the corresponding unsaturated population inversions. The coefficient κ is proportional to the stimulated emission cross-section. To take the partial overlap between the modes into account, we introduce the coefficients ξ_{12} and ξ_{21} which are the ratios of the cross- to self-saturation coefficients. Then,

$$C = \xi_{12}\xi_{21} \quad (5)$$

is the nonlinear coupling constant, as defined by Lamb [11].

The steady-state solutions of Eqs. (1-4) corresponding to the simultaneous oscillation of the two modes are as following

$$N_1 \equiv N_{\text{th1}} = \frac{1}{\kappa\tau_1}, \quad (6)$$

$$N_2 \equiv N_{\text{th2}} = \frac{1}{\kappa\tau_2}, \quad (7)$$

$$F_1 \equiv F_{10} = F_{\text{sat}} \frac{(r_1 - 1) - \xi_{12}(r_2 - 1)}{1 - C}, \quad (8)$$

$$F_2 \equiv F_{20} = F_{\text{sat}} \frac{(r_2 - 1) - \xi_{21}(r_1 - 1)}{1 - C}, \quad (9)$$

where $F_{\text{sat}} = \Gamma/\kappa$ is the saturation intensity and $r_1 = N_{01}/N_{\text{th1}}$, $r_2 = N_{02}/N_{\text{th2}}$ are the excitation ratios for the corresponding modes.

Now we want to calculate the fluctuations in F_1 and F_2 around their steady-state values F_{10} and F_{20}. Within the frequency range of interest (100 kHz-100 MHz), the dominant source of noise is the pump intensity fluctuations, which we model as

$$N_{01}(t) = \overline{N_{01}} + \delta N_{01}(t), \quad (10)$$

$$N_{02}(t) = \overline{N_{02}} + \delta N_{02}(t). \quad (11)$$

We introduce the small fluctuations in photon numbers and corresponding population inversions around their steady-state values due to pump intensity fluctuations in the following manner:

$$F_1(t) = F_{10} + \delta F_1(t), \quad (12)$$

$$F_2(t) = F_{20} + \delta F_2(t), \quad (13)$$

$$N_1(t) = N_{\text{th1}} + \delta N_1(t), \quad (14)$$

$$N_2(t) = N_{\text{th2}} + \delta N_2(t). \quad (15)$$

#178129 - $15.00 USD Received 16 Oct 2012; revised 14 Jan 2013; accepted 15 Jan 2013; published 28 Jan 2013

After substituting Eqs. (10-15) into Eqs. (1-4), we linearize the equations and then by Fourier transforming the photon number fluctuations, we get:

$$\delta\tilde{F}_1(f) = \frac{1}{\tau}\frac{\left[1/\tau_2 - \frac{2i\pi f}{\kappa F_{20}}(r_2/\tau - 2i\pi f)\right]\delta\tilde{N}_{01}(f) - \xi_{12}\delta\tilde{N}_{02}(f)/\tau_1}{\left[1/\tau_1 - \frac{2i\pi f}{\kappa F_{10}}(r_1/\tau - 2i\pi f)\right]\left[1/\tau_2 - \frac{2i\pi f}{\kappa F_{20}}(r_2/\tau - 2i\pi f)\right] - C/\tau_1\tau_2}, \quad (16)$$

$$\delta\tilde{F}_2(f) = \frac{1}{\tau}\frac{\left[1/\tau_1 - \frac{2i\pi f}{\kappa F_{10}}(r_1/\tau - 2i\pi f)\right]\delta\tilde{N}_{02}(f) - \xi_{21}\delta\tilde{N}_{01}(f)/\tau_2}{\left[1/\tau_2 - \frac{2i\pi f}{\kappa F_{20}}(r_2/\tau - 2i\pi f)\right]\left[1/\tau_1 - \frac{2i\pi f}{\kappa F_{10}}(r_1/\tau - 2i\pi f)\right] - C/\tau_1\tau_2}. \quad (17)$$

In our experiment, the two partially overlapping gain regions corresponding to the two modes are pumped with the same pump laser. We thus assume that the pump intensity fluctuations for the two modes have the same power spectral density and can be approximated as following :

$$\langle|\delta\tilde{N}_{01}(f)|^2\rangle = \langle|\delta\tilde{N}_{02}(f)|^2\rangle = \langle|\delta\tilde{N}_0|^2\rangle, \quad (18)$$

$$\langle\delta\tilde{N}_{01}(f)\delta\tilde{N}^*_{02}(f)\rangle = \eta\langle|\delta\tilde{N}_0|^2\rangle e^{i\psi}. \quad (19)$$

Equation (18) implies that the pump noises for the two modes are white noises of equal amplitude, as checked previously for the same type of pump laser [17], whereas Eq. (19) denotes the correlation between the pump intensity fluctuations for the two modes. We have assumed that the fluctuations of pump intensities for the two modes are partially correlated ($0 < \eta < 1$) because they do not fully overlap and that the correlation factor η is independent of frequency within the particular range of our interest (100 kHz-100 MHz). Moreover the fluctuations are supposed in phase ($\psi = 0$). The relative intensity noise (RIN) of the pump for the two modes can be written as

$$\mathrm{RIN}_{\mathrm{pump1}} = \frac{\langle|\delta\tilde{N}_0(f)|^2\rangle}{\overline{N_{01}}^2}, \quad (20)$$

$$\mathrm{RIN}_{\mathrm{pump2}} = \frac{\langle|\delta\tilde{N}_0(f)|^2\rangle}{\overline{N_{02}}^2}. \quad (21)$$

The expressions of the relative intensity noise (RIN) for the two modes can be written as

$$\mathrm{RIN}_1(f) = \frac{\langle|\delta\tilde{F}_1(f)|^2\rangle}{F_{10}^2}, \quad (22)$$

$$\mathrm{RIN}_2(f) = \frac{\langle|\delta\tilde{F}_2(f)|^2\rangle}{F_{20}^2}. \quad (23)$$

The normalized intensity noise correlation spectrum between the two modes is given as

$$\Theta(f) = \frac{\langle\delta\tilde{F}_1(f)\delta\tilde{F}^*_2(f)\rangle}{\sqrt{\langle|\delta\tilde{F}_1(f)|^2\rangle\langle|\delta\tilde{F}_2(f)|^2\rangle}}. \quad (24)$$

The correlation spectrum $\Theta(f)$ is a complex quantity with an amplitude and a phase. The correlation amplitude spectrum and correlation phase spectrum are given by $|\Theta|^2$ and $\mathrm{Arg}(\Theta)$, respectively. This quantity has to verify that $|\Theta(f)| \leq 1$. $|\Theta(f)| = 1$ means that the correlation is perfect at frequency f.

#178129 - $15.00 USD Received 16 Oct 2012; revised 14 Jan 2013; accepted 15 Jan 2013; published 28 Jan 2013

3. Experimental setup

Figure 2 shows the schematic of our experimental set-up. The laser operating at 1 μm, is based on 1/2-VCSEL gain structure, grown by Metal Organic Chemical Vapour Deposition (MOCVD) [18]. The SiC substrate having high thermal conductivity dissipates the extra heat generated by the pump on the 1/2-VCSEL structure to maintain a good efficiency. The temperature of the structure is maintained at 19^{o}C using a Peltier thermoelectric cooler which is fixed on a copper heat sink. The Bragg mirror with 99.9% reflectivity inside the 1/2-VCSEL structure contains 28 pairs of alternating GaAs/AlAs layers operating at 1 μm. Gain at 1 μm is provided by six strained balanced InGaAs/GaAsP quantum wells. The anti-reflection coating on the top of the structure is to reduce the residual Fabry-Perot effect between the Bragg mirror and the air-semiconductor interface. The gain structure is optically pumped with a 808 nm diode laser pigtailed with multimode fiber and delivering up to 3 W with an incidence angle of about 40^o. The length of the laser cavity is close to 1.5 cm and the cavity is closed with a concave mirror of radius of curvature 25 mm and reflectivity 99.5%. In these conditions, the photon lifetime is

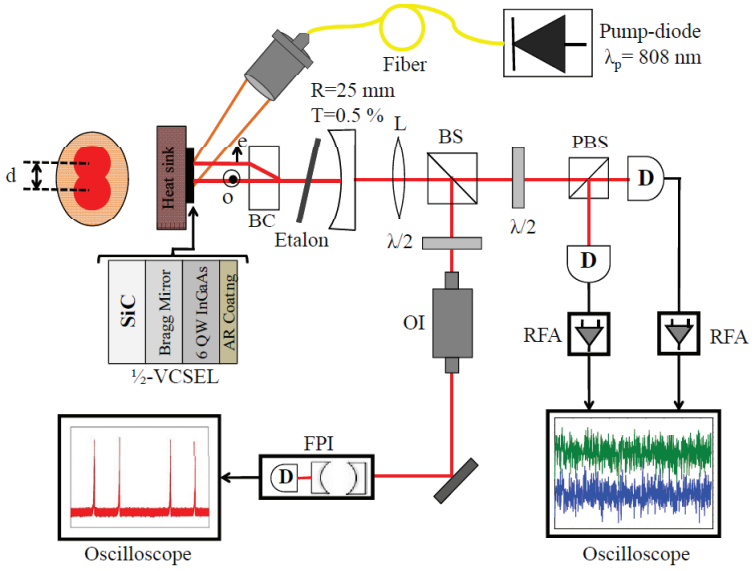

Fig. 2. Experimental setup used to study the intensity noise spectra and correlations. BC: birefringent crystal; R: radius of curvature of output coupler; T: transmittance of the output coupler; L: lens; BS: beam splitter; OI: optical isolator used to prevent unwanted feedback to the laser; FPI: Fabry-Perot interferometer; D: photodiode; PBS: polarization beam splitter; RFA: radio frequency amplifier. *d* represents the spatial separation between the two modes on the gain structure.

of the order of 10 ns, which is sufficiently longer than the carrier lifetime (of the order of 3 ns), thus ensuring class-A dynamical behaviour of the laser [19]. A birefringent YVO_4 crystal (BC) with anti-reflection coating at 1 μm, is introduced inside the cavity to obtain dual polarization oscillation. Since the semiconductor structure exhibits a linear gain dichroism, we orient the maximum gain axis along the bisector of the ordinary and extraordinary eigenpolarizations of the birefringent crystal. This birefringent crystal introduces a polarization walk-off *d* proportional to its thickness. The simultaneous oscillation of two perpendicularly linearly polarized

#178129 - $15.00 USD Received 16 Oct 2012; revised 14 Jan 2013; accepted 15 Jan 2013; published 28 Jan 2013

beams, which correspond to the ordinary and extraordinary polarization directions of BC, is achieved by reducing the coupling constant value below unity by spatially separating the two beams on the gain structure [13]. The diameter of the two laser modes is calculated to be about 62 μm. The size and the position of the pump spot are adjusted on the gain structure in such a way that the two modes are almost identically pumped. To vary the coupling strength, we have used three different thicknesses for BC, namely 1 mm, 0.5 mm, and 0.2 mm, which correspond to spatial separations d between the modes of 100 μm, 50 μm, and 20 μm, respectively. The perfect spatial overlapping of the beams in between BC and the cavity mirror M is ensured by the fact that M is concave while the Bragg mirror is planar. A 150-μm thick uncoated glass étalon is used to force each polarization to oscillate in a single longitudinal mode. The laser output is continuously analyzed with a 10 GHz free spectral range Fabry-Perot interferometer (FPI) followed by an oscilloscope to ensure that the two orthogonally polarized modes, which are longitudinally monomode, are always oscillating simultaneously in the laser cavity and that there is no mode hopping during the data acquisition. During the measurement we have also checked that no higher order transverse mode is oscillating for both the eigenpolarizations. The half-wave plate ($\lambda/2$) followed by the polarization beam splitter (PBS) in front of the detectors (Discovery DSC-30S, 22 GHz bandwidth) enable to separately detect the two orthogonally polarized modes on two identical detectors without mixing them. After amplifying the two RF signals by using RF amplifiers (Mini-circuits ZFL-1000LN+, bandwidth=1000 MHz, gain=20 dB, noise figure $\approx$ 2.9 dB), these signals are recorded simultaneously in time domain using a digital oscilloscope (sampling rate = 800 MSa/s, record length = 4,000,000 points) to measure intensity noise correlation. The modulus of the correlation amplitude is averaged over 6 different records, while the correlation phase is plotted for one record only.

4. Experimental and theoretical results

In our experiment the coupling between the two orthogonally polarized modes is varied by changing the spatial separation d with the help of birefringent crystal (BC). We have performed the noise correlation measurements for three different crystals of thickness 1 mm, 0.5 mm and 0.2 mm, which respectively correspond to the spatial separations of $d = 100$ μm, 50 μm and 20 μm on the gain structure. All the measurements reported here have been obtained for a pump power of about 1.5 W, and a laser output power of the order of 15 to 20 mW in each polarization. Figure 3 shows the experimental and theoretical results when the two orthogonally polarized modes are spatially separated by $d = 100$ μm (1 mm thick BC)). In this case, for the theoretical simulation, the coupling constant (C) value is taken as 0.1. This value has been calculated using Eq. (12) of Ref. [13] with the values of w_0 and d corresponding to our experimental conditions.The experimental relative intensity noise spectra (Fig. 3(a)) for the two modes are flat before the rolling off around 20-30 MHz due to limited bandwidth of the laser cavity. This first order filter like behavior, without any relaxation oscillation peak, confirms the class-A dynamical behavior of the laser [20]. It illustrates one more time how the intensity noise of the laser can be a good probe of the laser dynamics [21]. The red and blue curves in the RIN spectra are corresponding to the RINs of the two oscillating modes, which are not exactly identical because of slight difference of intra-cavity losses and gains for the two modes. This behavior is also theoretically reproduced by our model, as shown in Fig. 3(b). The experimentally measured noise correlation amplitude and correlation phase are shown in Figs. 3(c) and 3(e), respectively. As we can see, the noise correlation amplitude spectrum (Fig. 3(c)) is flat and equal to about -6 dB, and the correlation phase spectrum is also flat and remains always around 0 (Fig. 3(e)). This signifies that the intensity fluctuations of the two modes are partially correlated (0 dB would correspond to full correlation) and that the correlated part of the fluctuations are in phase. The decrease of the correlation amplitude above 20-30 MHz in

#178129 - $15.00 USD Received 16 Oct 2012; revised 14 Jan 2013; accepted 15 Jan 2013; published 28 Jan 2013

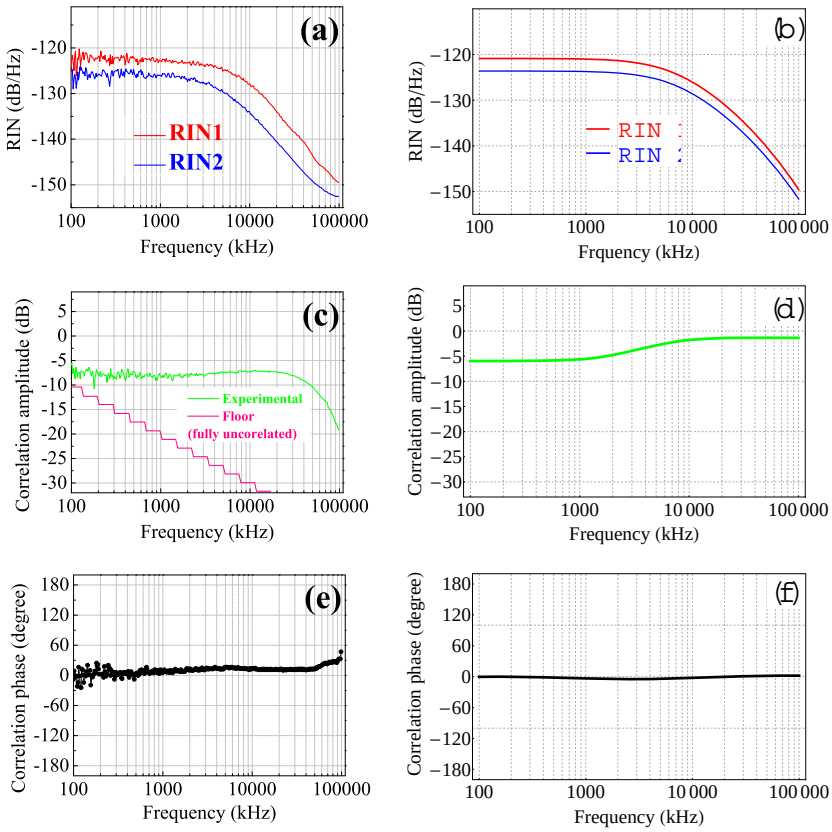

Fig. 3. Results for 1-mm thick crystal, which corresponds to a spatial separation $d = 100\ \mu$m between the modes. Relative intensity noise (RIN) spectra for the two oscillating modes: (a) experimental and (b) theoretical. Intensity noise correlation amplitude spectrum: (c) experimental and (d) theoretical. Intensity noise correlation phase spectrum: (e) experimental and (f) theoretical. Parameter values used for simulation: $C = \xi_{12}\xi_{21} = 0.1$; $r_1 = 1.3$, $r_2 = 1.4$; $\tau_1 \approx 5$ ns, $\tau_2 \approx 7$ ns; $\tau = 3$ ns; $\mathrm{RIN}_{\mathrm{pump}} = -135$ dB/Hz and $\eta = 0.85$.

the experimental spectrum as in Fig. 3(c) is due to the decrease of the RIN down to the technical noise level above these frequencies, and should not be taken into account. The staircase like pink curve in Fig. 3(c) is obtained by theoretical estimate of the minimum correlation that can be detected by our algorithm used to compute the correlation spectrum. Indeed, this algorithm averages the correlation amplitude over a number of samples which increases with the frequency. Thus, by supposing that the two signals are completely uncorrelated, the algorithm gives the level of correlation described by this pink line. The theoretical correlation amplitude and phase spectra are respectively shown in Fig. 3(d) and Fig. 3(f), which show nice agreement with the experiment. The values of r_1 and r_2 used to plot the theoretical curves of Fig. 3 have been estimated from the experiment (ratios of the pump power to threshold pump powers). The values of τ_1 and τ_2 have been adjusted and the value of τ has been extracted from preceding experiments performed with that active medium [20]. Notice also that we took white RIN spectra for the pump, which is compatible with our preceding observations in this frequency range [17].

Figure 4 shows the experimental and theoretical results for 0.5 mm thick crystal (BC), which

#178129 - $15.00 USD Received 16 Oct 2012; revised 14 Jan 2013; accepted 15 Jan 2013; published 28 Jan 2013

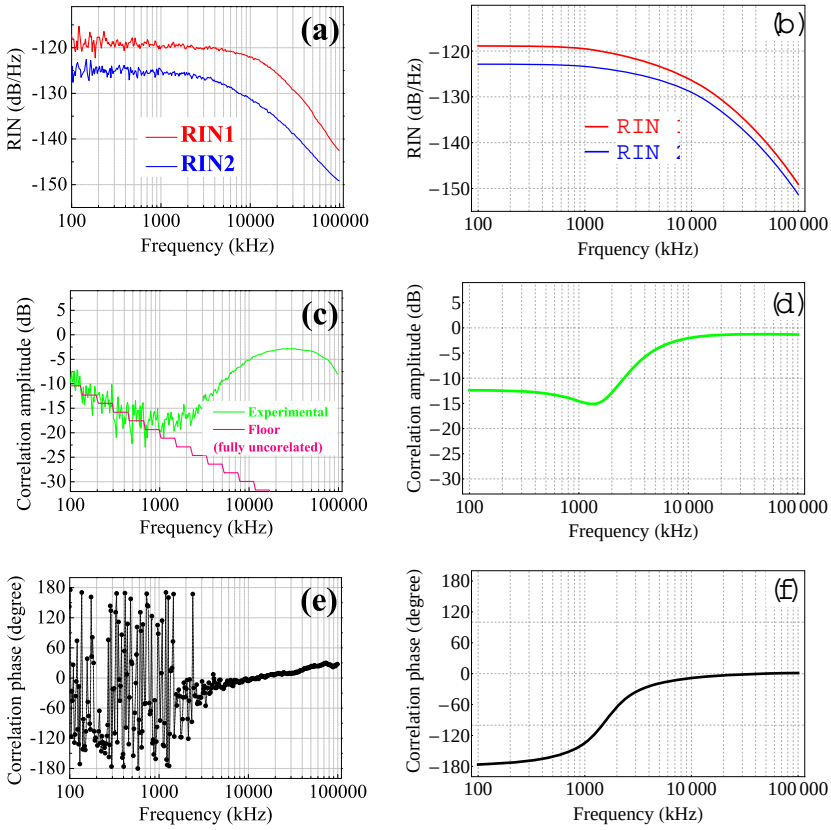

Fig. 4. Results for 0.5-mm thick crystal, which corresponds to a spatial separation $d = 50\ \mu$m between the modes. Relative intensity noise (RIN) spectra for the two oscillating modes: (a) experimental and (b) theoretical. Intensity noise correlation amplitude spectrum: (c) experimental and (d) theoretical. Intensity noise correlation phase spectrum: (e) experimental and (f) theoretical. Parameter values used for simulation: $C = \xi_{12}\xi_{21} = 0.35$; $r_1 = 1.4$, $r_2 = 1.48$; $\tau_1 \approx 5$ ns, $\tau_2 \approx 7$ ns; $\tau = 3$ ns; $\mathrm{RIN}_{\mathrm{pump}} = -135$ dB/Hz and $\eta = 0.85$.

corresponds to the spatial separation of $d = 50\ \mu$m on the gain structure, between the two orthogonally polarized modes. For theoretical simulation we have taken the value of 0.35 for the coupling constant C computed from Ref. [13]. Figure 4(a) shows the experimental RIN spectra for the two oscillating modes, which are not identical due to different intra-cavity losses and gains for the two modes. Because of the class-A dynamical behaviour of the laser, the RIN spectra are nearly flat without any relaxation oscillation peak before rolling off around 20-30 MHz due to limited bandwidth of the laser cavity. The corresponding theoretical RIN spectra are shown in Fig. 4(b) and show very good agreement with experiment. The experimental noise correlation amplitude and phase spectrum are shown in Fig. 4(c) and Fig. 4(e), respectively. As we can see in Fig. 4(c), the level of correlation is very low below 1-2 MHz and above this cut-off frequency the correlation gradually increases up to nearly -3 dB before it falls again after 20-30 MHz due to the reduction of the RIN down to technical noise level. Moreover in the correlation phase spectrum (Fig. 4(e)), the phase of correlation is undetermined below 1-2 MHz, whereas it is always around 0 above this frequency range. The theoretical spectra of correlation amplitude and phase are shown in Fig. 4(d) and Fig. 4(f) respectively, and are nicely

#178129 - $15.00 USD Received 16 Oct 2012; revised 14 Jan 2013; accepted 15 Jan 2013; published 28 Jan 2013

matching the corresponding experimental ones.

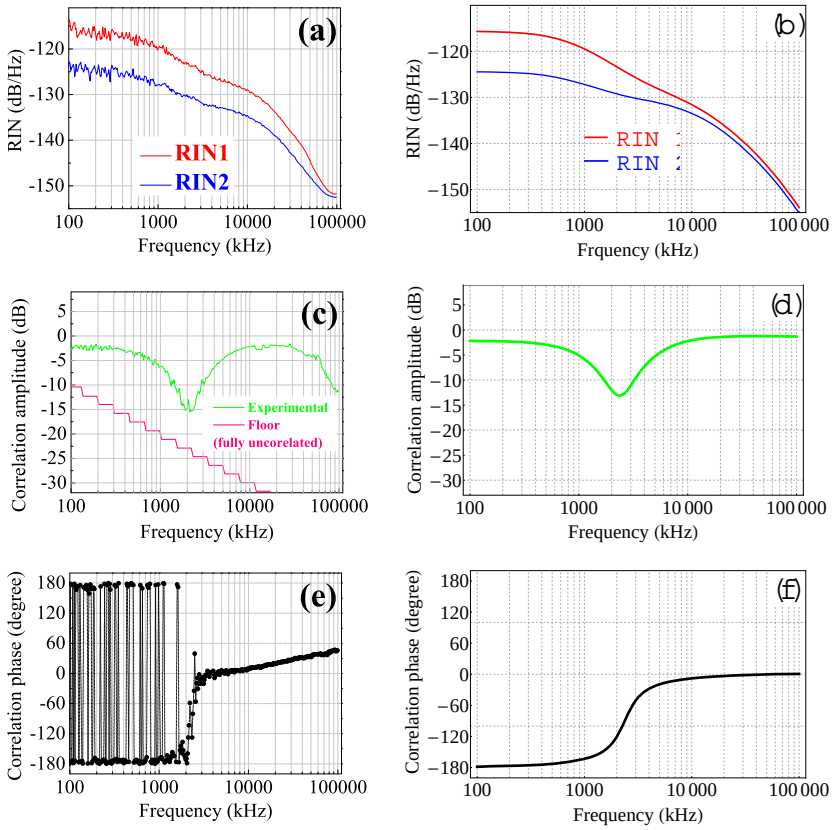

Fig. 5. Results for 0.2-mm thick crystal, which corresponds to a spatial separation $d = 20\ \mu$m between the modes. Relative intensity noise (RIN) spectra for the two oscillating modes: (a) experimental and (b) theoretical. Intensity noise correlation amplitude spectrum: (c) experimental and (d) theoretical. Intensity noise correlation phase spectrum: (e) experimental and (f) theoretical. Parameter values used for simulation: $C = \xi_{12}\xi_{21} = 0.65$; $r_1 = 1.45$, $r_2 = 1.5$; $\tau_1 \approx 5$ ns, $\tau_2 \approx 6$ ns; $\tau = 3$ ns; $\mathrm{RIN}_{\mathrm{pump}} = -135$ dB/Hz and $\eta = 0.85$.

Finally the experimental as well as the theoretical results for a 0.2 mm thick crystal (BC), which corresponds to a spatial separation of $d = 20\ \mu$m between the modes on the gain structure (corresponding to $C = 0.65$ [13]), are shown in Fig. 5. Figures 5(a) and 5(b) depict respectively the experimental and theoretical RIN spectra for the two oscillating modes, which show nice agreement between theory and experiment. The RIN spectra of the two modes are not exactly identical due to different intra-cavity losses and gains for the modes. There are no relaxation oscillation peaks in the RIN spectra, which confirms class-A dynamical behavior of the laser. But if we carefully look at the RIN spectra, a change of slope around 1-2 MHz is observed for both the experimental (Fig. 5(a)) and the theoretical (Fig. 5(b)) results. Now as we can see from the experimental correlation amplitude spectrum (Fig. 5(c)), there is a dip at about 1-2 MHz and apart from this dip the level of correlation is high (nearly -3 dB) except the falling above 20-30 MHz, which is again due to the very low level of RIN at these frequencies. The corresponding theoretical correlation amplitude spectrum as shown in Fig. 4(d), nicely matches with the experiment. Again Fig. 4(e) and Fig. 4(f) are the experimental and theoretical correlation

#178129 - $15.00 USD Received 16 Oct 2012; revised 14 Jan 2013; accepted 15 Jan 2013; published 28 Jan 2013

phase spectra, respectively, which also show nice agreement between experiment and theory. We see in the correlation phase spectra that the phase of correlation is always π below 1-2 MHz, whereas it is always 0 above this cut-off frequency.

5. Discussion

If we now compare the results of different coupling situations (1 mm, 0.5 mm and 0.2 mm thick BC respectively), then we find that the low frequency behaviors (below 1-2 MHz) of the noise correlation spectra as well as the RIN spectra are depending on the strength of coupling, whereas above this cut-off frequency the behaviors remain almost unchanged for different coupling situations. To explain this properly, it is important to explore the basic physical mechanism behind all these interesting results.

To start the explanation, let us recall the analogy between a single-frequency laser and a single mechanical oscillator (for example a mass attached to a spring). If this oscillator is pulled out of its steady-state, it will relax to its steady-state either exponentially or in damped-oscillatory manner depending on the level of damping. Similarly, a single-frequency laser relaxes to its steady-state intensity either exponentially or by exhibiting damped oscillations, depending on whether it is a class-A or class-B laser. If now we consider the case of two identical coupled oscillators, then the relaxation mechanism (either exponential or damped-oscillatory) of the whole system can be expanded along two mechanisms: (i) in-phase relaxation mechanism and (ii) anti-phase relaxation mechanism [22]. These two mechanisms, which are the eigenvectors of the linear dynamical equations governing the relaxation of the whole system, exhibit two different eigenfrequencies and/or damping rates. The dual-frequency laser, where the two orthogonally polarized coupled modes are oscillating, is the exact analog of the two coupled mechanical oscillator system. Again since our laser is class-A type, it will relax to its steady-state exponentially, not in damped-oscillatory manner (no relaxation oscillation). Moreover, since the two oscillating modes are coupled, analogous to the two-coupled mechanical oscillator system, there are two ways of relaxation either in-phase relaxation or anti-phase relaxation. The transfer functions of the in-phase and anti-phase response for three different coupling situations can be easily calculated and are shown in Fig. 6. In this figure, the blue and red curves correspond respectively to the transfer functions of in-phase response and anti-phase response for all coupling situations. As we can see in Fig. 6, the cut-off frequency of anti-phase response (around 1-2 MHz) is lower than the cut-off frequency of in-phase response (around 20-30 MHz).

Now, for small coupling (C = 0.1) as shown in Fig. 6(a), the in-phase response strongly dominates over the anti-phase response throughout the entire frequency range of our interest. So the noise of any one of the oscillating modes, obtained by subtracting the corresponding in-phase response from the anti-phase response, is determined mainly by the in-phase relaxation mechanism. But for high coupling (C = 0.65), the anti-phase response dominates below 1-2 MHz, but above this cut-off frequency, the in-phase response dominates. So the low frequency (below 1-2 MHz) behavior of noise spectrum of each laser mode is mainly determined by anti-phase relaxation mechanism, whereas for the high frequency (above 1-2 MHz) behavior, the main contribution comes from in-phase relaxation mechanism. Finally for intermediate coupling situation (C = 0.35), the contributions of in-phase and anti-phase relaxation mechanism to the noise spectrum are nearly comparable for low frequencies (below 1-2 MHz), but above this cut-off frequency the main contribution comes only from in-phase relaxation mechanism. So the low frequency behavior (below 1-2 MHz) of the noise spectrum of each mode varies with the variation of the coupling strength, since the anti-phase response which has a lower cut-off frequency than the in phase-response depends on coupling strength. Besides, the in-phase response is almost independent of the coupling and has higher cut-off frequency than the anti-phase response.

#178129 - $15.00 USD Received 16 Oct 2012; revised 14 Jan 2013; accepted 15 Jan 2013; published 28 Jan 2013

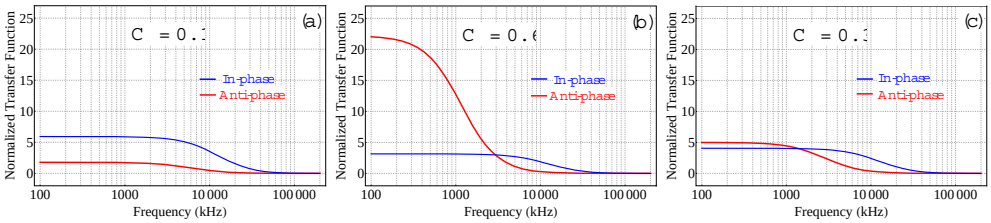

Fig. 6. The theoretical normalized transfer function for both in-phase and anti-phase relaxation mechanism for three different values of coupling (a) $C = 0.1$, (b) $C = 0.65$ and (c) $C = 0.35$. The other parameters used for the simulation: $r_1 = r_2 = 1.5$; photon lifetimes for the two modes inside the cavity: $\tau_1 = \tau_2 = 5$ ns; population inversion lifetime: $\tau = 3$ ns; pump noise correlation factor: $\eta = 0.85$.

With this physical reasoning we can perfectly explain our results of intensity noise correlation spectra as well as the RIN spectra for different coupling situations. For the first case of 1 mm thick BC as shown in Fig. 3, which corresponds to a spatial separation of 100 μm between the modes on the gain structure, the coupling between the modes is very low ($C = 0.1$). So the two oscillating modes behave almost as two independent lasers and the intensity fluctuations of the two modes which are mainly due to pump intensity fluctuations, are also independent. So the RIN spectra of the two modes are like of two independent lasers of class-A type as shown in Figs. 3(a, b). But since the two modes are pumped by the same pump and the pump intensity fluctuations for the two modes are assumed to be identical in amplitude and phase ($\psi = 0$) and partially correlated, the intensity fluctuations of the two-modes are also partially correlated (nearly -6 dB as in Figs. 3(c, d)) and are also in phase (0 correlation phase as in Figs. 3(e, f)). Now for another extreme case of 0.2 mm thick crystal, which corresponds to a spatial separation of 20 μm between the modes on the gain structure, the strength of coupling is significantly higher ($C = 0.65$). Here the low frequency behavior (below 1-2 MHz) of the RIN spectrum of each mode is mainly determined by anti-phase relaxation mechanism, whereas above this cut-off frequency the main contribution in the noise spectrum of each mode comes from in-phase relaxation mechanism. So in the RIN spectrum of each laser mode, which is obtained by subtracting the anti-phase response from in-phase response for the corresponding mode, we find a change of slope near 1-2 MHz due to transition from strong anti-phase to strong in-phase relaxation mechanism. This is shown in Figs. 5(a, b). The π phase of the noise correlation below 1-2 MHz is due to dominating anti-phase mechanism. Above this cut-off frequency, the phase of the noise correlation is 0 because of dominating in-phase mechanism, as in Figs. 5(e, f). Moreover, due to the phase jump from π to 0 near 1-2 MHz, the fluctuations of the intensities of the two modes which are nearly identical in amplitude interfere destructively, giving rise to the dip around 1-2 MHz in the correlation amplitude spectrum. Apart from the dip, the correlation is high (nearly -3 dB) because of strong competition between the modes due to high coupling. This is shown in Figs. 5(c,d). Finally, in the case of the 0.5 mm thick crystal, for which the spatial separation between the two modes on the gain structure is 50 μm, the strength of coupling ($C = 0.35$) is intermediate between two previously mentioned extreme cases of 1 mm and 0.2 mm thick BC. Now since the coupling is not very strong the anti-phase relaxation mechanism is also not so dominant, whereas in-phase mechanism remains unchanged in all coupling situations. So we can no longer clearly distinguish any change of slope in the RIN spectra as shown in Figs. 4(a,b). Again below 1-2 MHz the in-phase and anti-phase responses are comparable, but above this cut-off frequency in-phase relaxation mechanism strongly dominates over anti-phase relaxation mechanism. As a result, the noise correlation phase is indeterministic below 1-2 MHz but always 0 for higher frequency values as shown in Fig. 5(e,f). Moreover

#178129 - $15.00 USD Received 16 Oct 2012; revised 14 Jan 2013; accepted 15 Jan 2013; published 28 Jan 2013

the correlation is very low up to 1-2 MHz, but above this cut-off frequency the amplitude of correlation is high (nearly -3 dB).

6. Conclusion

We have shown both experimentally and theoretically that the intensity fluctuations for the two orthogonally polarized modes in a dual frequency VECSEL are partially correlated (less than 0 dB) although the two modes are pumped by the same pump source and oscillating inside the same cavity. Moreover, we have explored the dependence of intensity noise correlation spectra on the strength of coupling between the modes. The theoretical model based on simple rate equations, which is developed on simple assumptions of partially correlated pump intensity fluctuations of identical amplitude, shows nice agreement with the experiment. One interesting prospect consists in using the more general model based on spin flip mechanism [14–16] and to extend it in order to take the partial spatial separation of the modes into account. Now as the phase noises are related to intensity noises due to high Henry factor of the semiconductor gain medium of our VECSEL [23, 24], we expect also to see the consequent effect of variation of coupling strength on the RF-beat note spectrum, which is obtained by optically mixing of the two orthogonollay polarized modes. So this leads to the future experiment of measuring RF beat-note spectrum for different coupling situations and also to measure the RF phase noise. This will help to improve the purity of the RF-beat note, which is prime interest for RADAR technology. Moreover since this noise correlation study is very general, this idea can also be extended to other kind of dual frequency lasers like as dual frequency solid-state lasers [3].

Acknowledgment

One of the authors (VP) thanks to the Council of Scientific and Industrial Research (CSIR) India for the financial support. This work was partially supported by the Agence Nationale de la Recherche (Project NATIF No. ANR-09-NANO-012-01). RG wishes to thank Université Paris Sud 11 for a CNRS invited researcher position.

#178129 - $15.00 USD Received 16 Oct 2012; revised 14 Jan 2013; accepted 15 Jan 2013; published 28 Jan 2013